the plant journal

SEB SOCIETY FOR EXPERIMENTAL BIOLOGY

The Plant Journal (2023) doi: 10.1111/tpj.16098

Leaf anatomy does not explain the large variability of mesophyll conductance across C_3 crop species

Dongliang Xiong*

National Key Laboratory of Crop Genetic Improvement, Hubei Hongshan Laboratory, MOA Key Laboratory of Crop Ecophysiology and Farming System in the Middle Reaches of the Yangtze River, Huazhong Agricultural University, Wuhan, Hubei, 430070, China

Received 27 March 2022; revised 29 December 2022; accepted 2 January 2023.
*For correspondence (e-mail dlxiong@mail.hzau.edu.cn).

SUMMARY

Increasing mesophyll conductance of CO_2 (g_m) is a strategy to improve photosynthesis in C_3 crops. However, the relative importance of different anatomical traits in determining g_m in crops is unclear. Mesophyll conductance measurements were performed on 10 crops using the online carbon isotope discrimination method and the 'variable *J*' method in parallel. The influences of crucial leaf anatomical traits on g_m were evaluated using a one-dimensional anatomical CO_2 diffusion model. The g_m values measured using two independent methods were compatible, although significant differences were observed in their absolute values. Quantitative analysis showed that cell wall thickness and chloroplast stroma thickness are the most important elements along the diffusion pathway. Unexpectedly, the large variability of g_m across crops was not associated with any investigated leaf anatomical traits except chloroplast thickness. The g_m values estimated using the anatomical model differed remarkably from the values measured *in vivo* in most species. However, when the species-specific effective porosity of the cell wall and the species-specific facilitation effect of CO_2 diffusion across the membrane and chloroplast stoma were taken into account, the model could output g_m values very similar to those measured *in vivo*. These results indicate that g_m variation across crops is probably also driven by the effective porosity of the cell wall and effects of facilitation of CO_2 transport across the membrane and chloroplast stroma in addition to the thicknesses of the elements.

Keywords: crops, cell wall porosity, mesophyll conductance, leaf anatomy, photosynthesis.

INTRODUCTION

The photosynthetic rate of C_3 plants is proposed to be strongly restricted by the partial CO_2 pressure at carboxylation sites in the chloroplast stroma (Barbour et al., 2010; Evans & von, 1996; Flexas et al., 2016; Gago et al., 2019). The diffusion-driven conductance of CO_2 from the atmosphere to chloroplasts inside leaves, which has been described using Fick's first law of diffusion, mainly consists of stomatal conductance (g_s) and mesophyll conductance (g_m) in series (Barbour, 2017; Evans & von Caemmerer, 1996; von Caemmerer, 2000). Stomatal conductance can be quantified based on the leaf water vapor flux because water and CO_2 share the same gaseous diffusion pathway via stomata. It is highly regulated by stomatal opening/closing dynamics (von Caemmerer & Farquhar, 1981). Mesophyll conductance is defined as the diffusion efficiency of CO_2 molecules from the intercellular air space to chloroplasts. The pathway is more complex since molecular CO_2 must move through different cell components, including cell walls, membranes, and the cytoplasm, before entering chloroplasts, where photosynthesis takes place (Evans, 2021; Flexas et al., 2012; Tomás et al., 2013; Tosens, Niinemets, Vislap, et al., 2012). In C_3 plants, g_m is roughly similar in magnitude to g_s and accounts for about half of the leaf CO_2 diffusion resistance (Flexas et al., 2013; Xiong et al., 2017, 2018).

Currently, g_m is widely estimated with methods that are not straightforward and require a series of assumptions and multiple input variables (Gu & Sun, 2014; Pons et al., 2009). The online carbon isotope discrimination method (Evans et al., 1986; Lloyd et al., 1992) and the 'variable *J*' method based on leaf chlorophyll fluorescence (Harley et al., 1992) are the most widely used methods for g_m estimation (Flexas et al., 2018; Lundgren & Fleming, 2020). In the last decades, g_m and its responses to environmental conditions have been widely estimated for many species (summarized by Flexas et al., 2018). These estimations revealed that g_m varies significantly among

species and environmental conditions, such as light, CO_2, temperature, and nutrients, although determinants and regulatory mechanisms of g_m are not fully understood (Cousins et al., 2020; Evans, 2021; Flexas et al., 2018; Gago et al., 2019; Wang et al., 2018).

The rapid response of g_m to environmental conditions has been suggested to be mainly regulated by biochemical factors, including aquaporins and carbonic anhydrases (CAs; Barbour, 2017; Barbour & Kaiser, 2016; Cousins et al., 2020; Evans, 2021; Griffiths & Helliker, 2013; Huang et al., 2021; Lundgren & Fleming, 2020; von Caemmerer & Evans, 2015; Xiong et al., 2015). However, the variation of g_m across species is expected to be related to leaf anatomical characteristics (Carriquí et al., 2020; Clarke et al., 2021; Clemente-Moreno et al., 2019; Gago et al., 2019). The mesophyll cell wall thickness (T_{cw}) and the total chloroplast surface area exposed to mesophyll intercellular air spaces (S_c) per leaf area are two principal anatomical traits explaining g_m variations across species (Ellsworth et al., 2018; Evans, 1999; Flexas et al., 2021; Roig-Oliver et al., 2020; Sonawane et al., 2021; Sugiura et al., 2020; Tosens, Niinemets, Vislap, et al., 2012; Veromann-Jürgenson et al., 2020).

By assuming that g_m is composed of the partial conductance of each element, one-dimensional (1D) anatomical models were established and widely used in previous studies, although a few recent studies have suggested that three-dimensional (3D) anatomical models should be used (Borsuk et al., 2022; Earles et al., 2018; Harwood et al., 2020; Théroux-Rancourt & Gilbert, 2017). The modeled g_m values were correlated with the values estimated by the chlorophyll fluorescence method or the carbon isotope discrimination method *in vivo* in some studies (Tomás et al., 2013; Tosens, Niinemets, Vislap, et al., 2012) but not in others (Carriquí et al., 2019; Xiong & Flexas, 2021). The 1D anatomical CO_2 diffusion model is a pure physics-law-based model relying on the thicknesses of each cellular component extracted from microscopic images and several assumed parameters (see Evans et al., 2009 for details). Elements of uncertainty exist for almost all input parameters. For instance, the membrane permeability to CO_2 was set to 0.0035 m sec^{-1}, the value measured for a non-biological lecithin–cholesterol membrane, and the effective porosity values of cell walls and other cellular components were assumed to be constant across species. However, many studies highlighted that the CO_2 permeability of biological membranes is enhanced by aquaporins (reviewed by Groszmann et al., 2017), and the effective porosity of cell walls can be modified by changing the cell wall composition (Ellsworth et al., 2018; Flexas et al., 2021; Roig-Oliver et al., 2020). Moreover, CO_2 diffusion in each cellular component can also be facilitated by other factors, including the pH, CA activity, and the concentration and distribution of Rubisco in the chloroplast stroma (Mizokami et al., 2022).

Improving crop yield has significant social, economic, and environmental impacts, and photosynthesis is the primary determinant of crop yield (Long et al., 2006; Xiong et al., 2022). In crops with C_3 photosynthesis, increasing g_m is proposed to improve the efficiency of photosynthesis and water use in parallel (Barbour, Bachmann, et al., 2016; Flexas et al., 2012, 2013, 2016). Unfortunately, most of the traits determining g_m in C_3 crop plants are unknown. However, a recent study showed that g_m was manipulated in Arabidopsis mutants with modified anatomical features (Mizokami et al., 2019). Plants have evolved mechanisms to regulate the tradeoff between stress responses and productivity (Veromann-Jürgenson et al., 2020). For instance, the global leaf economics spectrum suggests that leaf anatomical traits such as T_{cw} and S_c mediate the tradeoff between stress responses and productivity (Onoda et al., 2017). Still, crop plants may have experienced tradeoffs during domestication as breeders selected for traits related to fast growth and high productivity (Milla et al., 2015).

Nevertheless, the effects of leaf anatomy and mesophyll structure on g_m have been studied in very few C_3 crop plants. Detailed knowledge about the leaf anatomical traits contributing to g_m variability across crop plants is necessary to improve crop photosynthesis. Therefore, this study aims to (i) quantify the variation of g_m across crops and its limiting effects on photosynthesis and (ii) elucidate the contribution of leaf anatomical traits to g_m variation among crop plants.

RESULTS

Variability in photosynthetic rate, stomatal conductance, and mesophyll conductance across crops

Substantial variations in photosynthetic rate (A), maximum carboxylation rate (V_{cmax}), electron transport rate (ETR), stomatal conductance (g_s), and mesophyll conductance (g_m) across C_3 crops were observed (Figure 1; Figure S3; Table S3). Across all selected crops, a 5.0-fold variation was found for A, a 3.7-fold variation was found for V_{cmax}, a 3.5-fold variation was found for ETR, and a 3.5-fold variation was found for g_s; moreover an 8.3-fold variation was found for g_m using the 'variable J' method (g_m_fluo) and a 3.5-fold variation was found for g_m using the online isotope method (g_m_$\Delta^{13}C$). *Helianthus annuus* had the highest A (44.6 μmol m^{-2} sec^{-1}), V_{cmax} (155.3 μmol m^{-2} sec^{-1}), ETR (350.7 μmol m^{-2} sec^{-1}), g_s (0.69 mol m^{-2} sec^{-1}), g_m_fluo (0.66 mol m^{-2} sec^{-1}), and g_m_$\Delta^{13}C$ (0.90 mol m^{-2} sec^{-1}), while the lowest A (11.6 μmol m^{-2} sec^{-1}), V_{cmax} (42.1 μmol m^{-2} sec^{-1}), ETR (99.2 μmol m^{-2} sec^{-1}), g_m_fluo (0.08 mol m^{-2} sec^{-1}), and g_m_$\Delta^{13}C$ (0.26 mol m^{-2} sec^{-1}) were recorded in *Lycopersicon esculentum*. Interestingly, *Solanum tuberosum* had the lowest g_s (0.20 mol m^{-2} sec^{-1}). As shown in Figure 2, the g_m values estimated using two

independent methods were well correlated (r^2 = 0.8; $P < 0.001$). Although the g_m values estimated using the online isotope method were significantly higher than the values estimated using the 'variable *J*' method (the intercept of the regression line was higher than 0), the slope of the regression line was very close to 1 (Figure 2). Across the investigated crops, strong pairwise correlations were observed between *A* and g_s (r^2 = 0.82; $P < 0.001$), g_m_fluo (r^2 = 0.84; $P < 0.001$), or g_m_Δ^{13}C (r^2 = 0.87; $P < 0.001$; Figure 3). The relative photosynthesis limitation analysis showed that photosynthesis was mainly limited by biochemical factors (Figure 3d). On average, the stomatal conductance (g_s), mesophyll conductance (g_m), and photosynthetic biochemical factors contributed 20.0% (from 11.0 to 30.4%), 22.2% (from 17.0 to 39.1%), and 57.8% (from 46.2 to 67.5%) of the limitation to photosynthesis, respectively.

Variation of leaf anatomical traits across crops

The intercellular air space fraction (f_{IAS}), mesophyll cell wall thickness (T_{cw}), chloroplast thickness (T_{chl}), mesophyll cell surface area facing the intercellular air space (S_m), and chloroplast surface area facing the intercellular air space (S_c) varied 1.6-fold, 3.0-fold, 1.9-fold, 1.5-fold, and 1.6-fold, respectively (Figure S4; Table S3). The roles of leaf anatomical traits in determining the variation of mesophyll conductance (g_m) across crop species were further investigated. Unexpectedly, no correlation was observed between mesophyll conductance (neither g_m_fluo nor g_m_Δ^{13}C) and the estimated leaf anatomical traits (i.e., f_{IAS}, T_{cw}, S_m, and S_c) except for T_{chl}. A negative correlation between g_m_fluo and T_{chl} was observed across species (r^2 = 0.33; $P < 0.001$; Figure 4). Mesophyll conductance (g_m) was also not significantly correlated to the ratio of S_c to leaf density (S_c/LD) across species (Figure S5a).

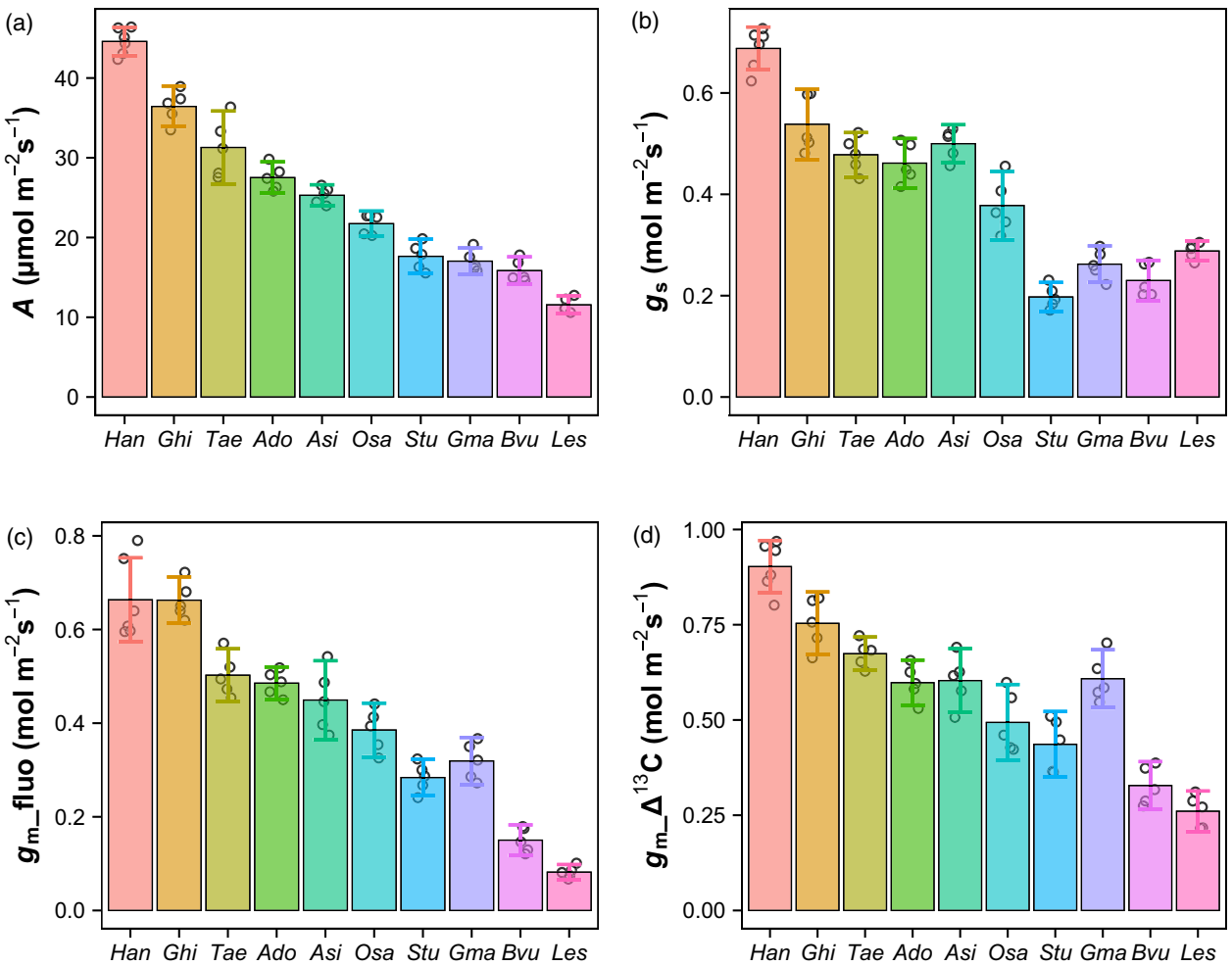

Figure 1. Photosynthetic characteristics of the crop species.
(a) Photosynthetic rate (*A*). (b) Stomatal conductance (g_s). (c) Mesophyll conductance estimated using the 'variable *J*' method (g_m_fluo). (d) Mesophyll conductance estimated using the online Δ^{13}C method (g_m_Δ^{13}C). Bars represent means (±SE, n = 5–6) values; open points represent pooled data for each species. All traits showed significant variation across species ($P < 0.05$, ANOVA, Table S2). The species nomenclature of abbreviations is provided in Table S1.

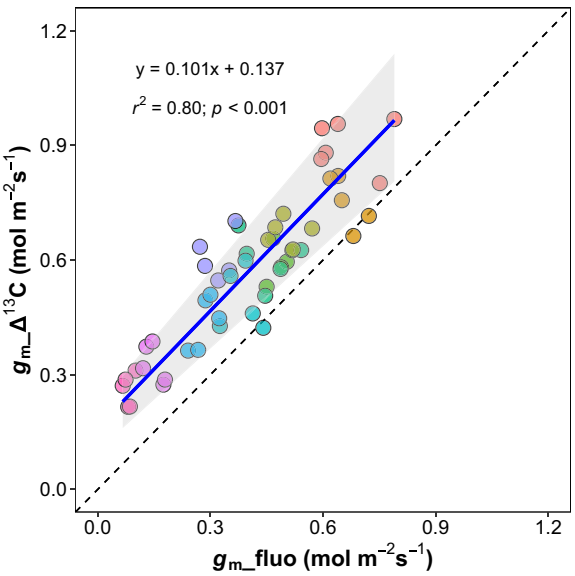

Figure 2. Standardized major axis (SMA) regression of the relationships between mesophyll conductance for all species measured using the online carbon isotope discrimination (g_m_Δ^{13}C) and 'variable *J*' (g_m_fluo) methods. Blue line, SMA regression; black dot line, 1:1 line; gray area, 95% confidence interval of the SMA regression. The slope of the SMA regression line does not differ from 1 (P = 0.79), but the intercept of the SMA regression line significantly differs from 0 (P < 0.001).

Using the measured leaf anatomical traits, mesophyll conductance was modeled by the 1D anatomical model and compared with estimated values by *in vivo* methods. If the effective porosity (ρ_i/τ_i) and the facilitation effects (ε) were set as constants in the model, the mesophyll conductance values estimated using the 1D anatomical model (g_m_anatomy) differed remarkably from the values estimated using the 'variable *J*' method or the online isotope method (Figure 5). The average values of g_m_anatomy varied from only 0.149 mol m^{-2} sec^{-1} (*Beta vulgaris*) to 0.244 mol m^{-2} sec^{-1} (*Gossypium hirsutum*). The value of g_m_anatomy was significantly correlated with g_m_fluo (r^2 = 0.20; P = 0.001) and g_m_Δ^{13}C (r^2 = 0.17; P = 0.003), although the r^2 values were quite low (Figure 5). Moreover, the slopes and intercepts of the regression lines were different from unity. The limitations of mesophyll conductance due to individual components of the diffusion pathway were also estimated (Figure 6). The gas phase resistance was lower (from 7.9 to 33.4%) than the liquid phase resistance. In liquid phase diffusion, the chloroplast stroma (from 40.5 to 67.8%) and the cell wall (from 15.4 to 40.9%) were the top two causes of resistance to CO_2 diffusion, and the resistance of the cytosol was the lowest (2.6–5.4%).

The variation of cell wall ρ_i/τ_i was suggested to be an important parameter influencing g_m_anatomy but was not considered in the model. As variation in cytosol and stroma thickness is independent of cell wall traits, a constant value for non-cell wall resistance can be assumed in the model. Therefore, different ρ_i/τ_i values were fitted to the dataset. The results showed that ρ_i/τ_i was species-dependent (Figure S5b). Further analysis revealed that species-dependent facilitation effects (ε) must be used as an input parameter in the model to obtain g_m_anatomy values comparable to those measured *in situ* (Figure 7).

DISCUSSION

Mesophyll conductance estimated using the 'variable *J*' and online isotope determination methods

Although recent interest in mesophyll conductance of CO_2 (g_m) has revealed one of the three crucial factors limiting photosynthesis, strong method biases exist in g_m estimation, as raised by several studies (Barbour, Evans, et al., 2016; Gu & Sun, 2014; Pons et al., 2009). There are many methods available for g_m estimation, including combining gas exchange measurements with online carbon isotope discrimination (Evans et al., 1986), oxygen isotope discrimination (Barbour, Evans, et al., 2016; Barbour, 2017), or chlorophyll fluorescence measurements (Harley et al., 1992), the CO_2 response curve fitting method (Ethier & Livingston, 2004; Sharkey et al., 2007), and 1D leaf anatomy-based modeling (Tomás et al., 2013; Tosens, Niinemets, Vislap, et al., 2012). All the currently available methods are based on specific assumptions and have their own limitations (Gu & Sun, 2014; Pons et al., 2009). In the literature, g_m is mostly estimated by two methodologies, combining gas exchange measurements with either online carbon isotope discrimination or chlorophyll fluorescence (Elferjani et al., 2021; Gago et al., 2019). Surprisingly, the g_m measurements using these two methods were rarely compared directly (Cano et al., 2014; Flexas et al., 2016; Théroux-Rancourt & Gilbert, 2017). To the best of my knowledge, the present study is the first to compare g_m values measured on the same leaf using both online carbon isotope discrimination (g_m_Δ^{13}C) and chlorophyll fluorescence (g_m_fluo) methods in parallel. As shown in Figure 2, the g_m_Δ^{13}C values were consistently higher than the g_m_fluo values and the two sets of values were linearly correlated with a slope very close to one. These results demonstrate that with simple calibration, the g_m_Δ^{13}C and g_m_fluo are compatible. However, the reasons leading to higher g_m values measured using the online carbon isotope method than the ones measured using the chlorophyll fluorescence method in the present study are unclear and require further investigation.

Mesophyll conductance and photosynthesis improvement in C_3 crops

Photosynthetic assimilation of CO_2 is the primary determinant of crop yield (Long et al., 2006). The current study

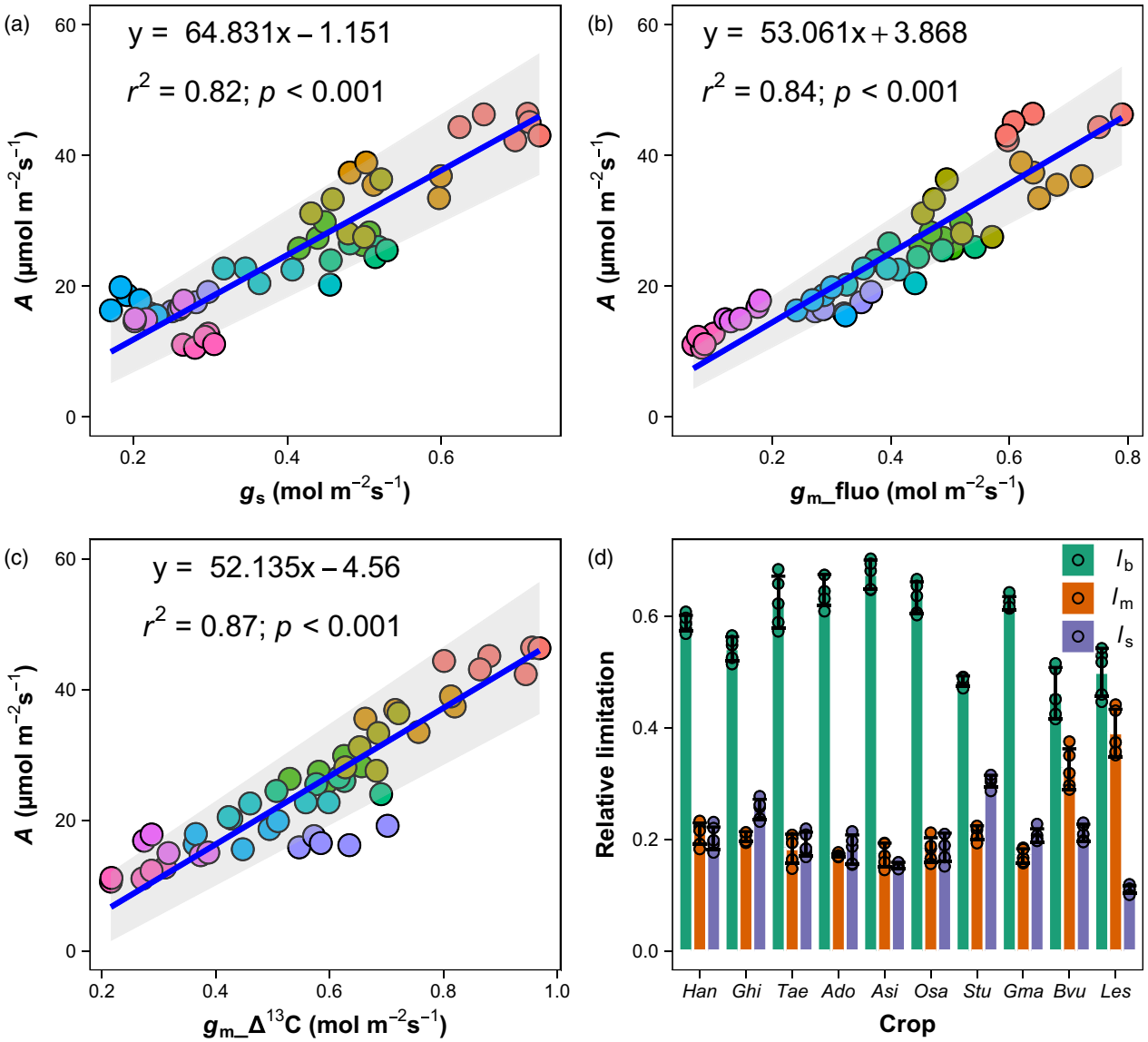

Figure 3. Correlations between photosynthetic rate (A) and CO_2 diffusion conductance.
(a) A versus stomatal conductance (g_s). (b) A versus mesophyll conductance estimated using the 'variable J' method (g_m_fluo). (c) A versus mesophyll conductance estimated using the online isotope method (g_m_Δ^{13}C). (d) Quantitative limitation analysis. The total relative limitation (1.0) of photosynthesis is the sum of biochemical (l_b), mesophyll conductance (l_m), and stomatal conductance (l_s) limitations. Blue lines represent the standardized major axis (SMA) regression lines; the gray areas are 95% confidence intervals of the SMA regression lines. In (d), bars represent mean (±SE, n = 5–6) values, and open points represent pooled data for each species.

showed that photosynthesis in crops is primarily limited by photosynthetic biochemistry, as it contributed about 60% of the photosynthesis limitation (Figure 3). Indeed, some recent studies also revealed that in plants with high photosynthetic capacity, like crops, photosynthesis is mainly limited by biochemistry and suggested that more efforts are needed to improve light and carbon conversion in crops to enhance photosynthesis (Gago et al., 2019; Nadal & Flexas, 2019). Coincidentally, Zhu et al. (2022) provided a list of opportunities to improve photosynthetic efficiency in crops, and most of them are related to photochemistry and biological CO_2 fixation processes. Although many studies suggested that both g_s and g_m are major photosynthetic limitations, most studies were conducted on non-crop plants with relatively low photosynthetic rates (Gago et al., 2019; Nadal & Flexas, 2019; Niinemets, Díaz-Espejo, et al., 2009; Niinemets, Wright, & Evans, 2009; Veromann-Jürgenson et al., 2020). The present analysis showed that CO_2 diffusion conductance contributed about 42% of photosynthetic limitations in crops, and further

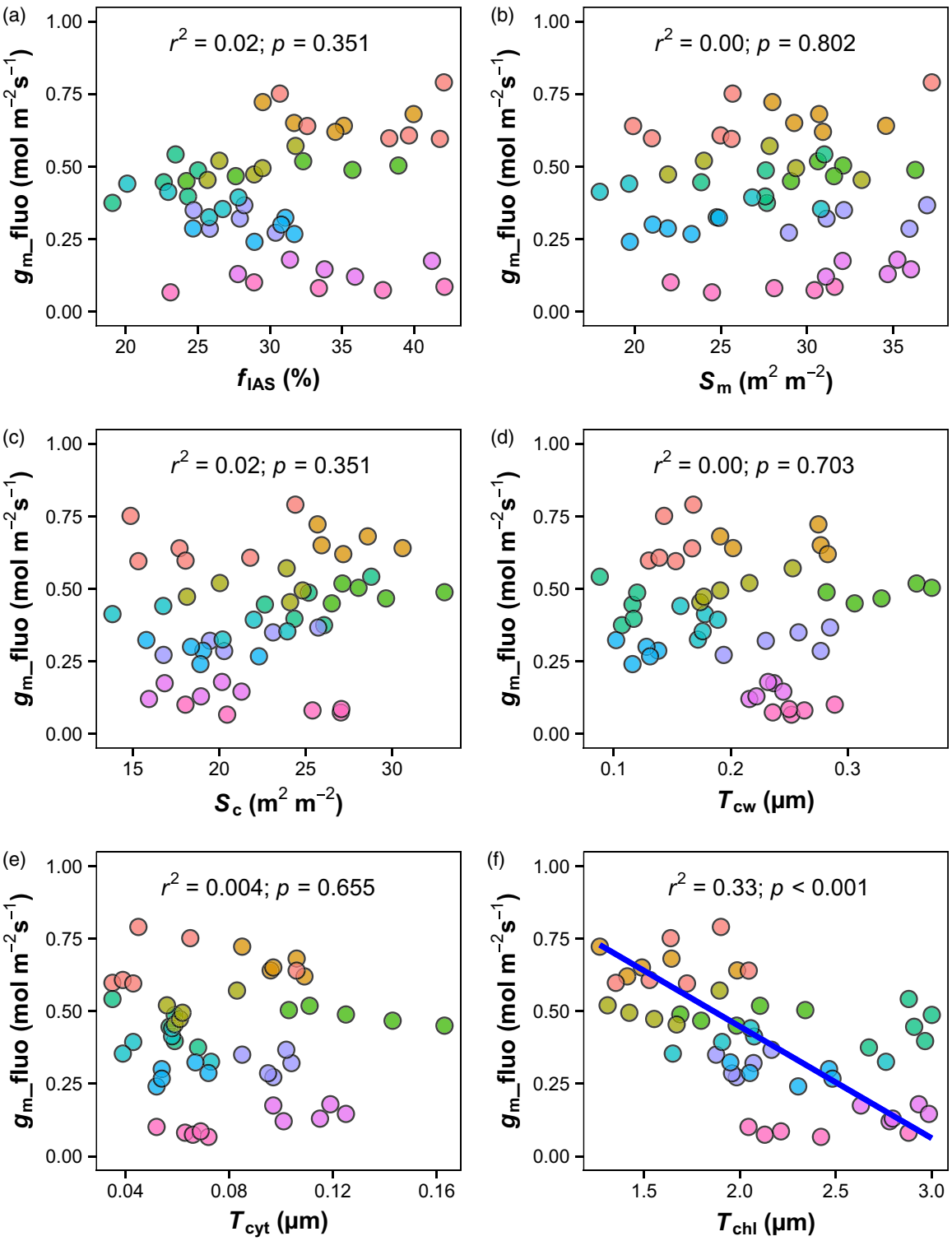

Figure 4. Relationships between mesophyll conductance and leaf anatomical traits.
(a) Intercellular air apace (f_{IAS}). (b) Cell wall thickness (T_{cw}). (c) Mesophyll cell surface facing the intercellular air space (S_m). (d) Chloroplast surface facing the intercellular air space (S_c). (e) Cytosol thickness (T_{cyt}). (f) Chloroplast stroma thickness (T_{chl}). The blue line is the standardized major axis (SMA) regression line.

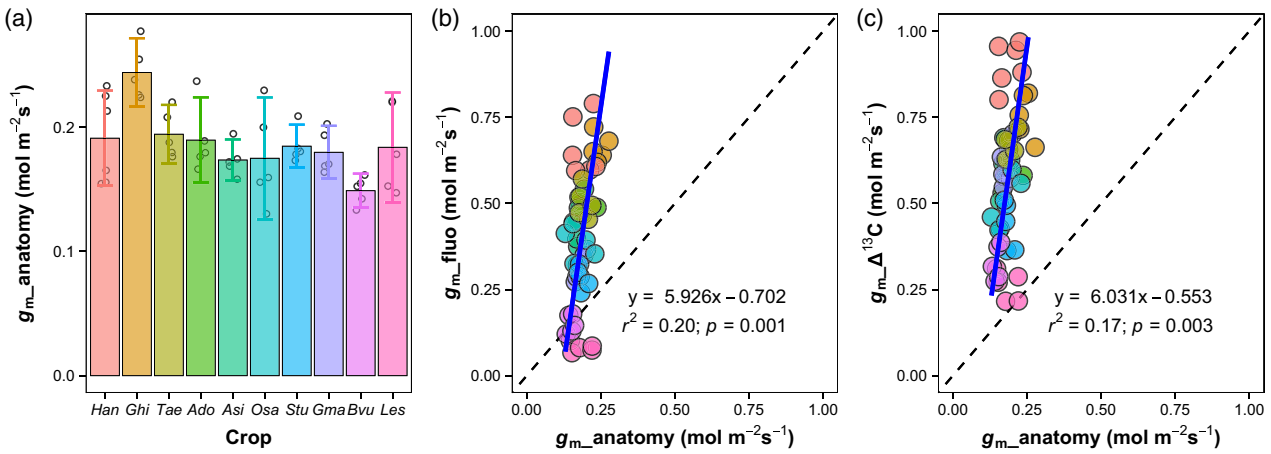

Figure 5. Modeled mesophyll conductance and its correlation with measured mesophyll conductance. (a) Mesophyll conductance modeled using leaf anatomical parameters (g_m_anatomy).
(b) Standardized major axis (SMA) regression analysis of the relationship between mesophyll conductance measured using the 'variable *J*' (g_m_fluo) method and g_m_anatomy. (c) SMA regression analysis of the relationship between the mesophyll conductance measured using the online carbon isotope discrimination (g_m_Δ^{13}C) method and g_m_anatomy. Blue lines are SMA regression lines, and the black dot line is the 1:1 line.

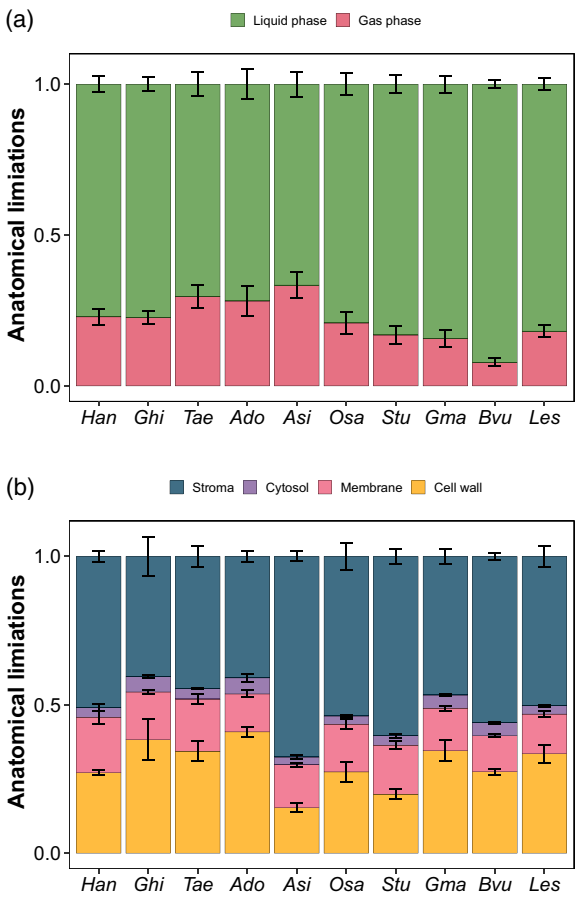

Figure 6. Limitation of mesophyll conductance due to anatomical constraints in 10 crops.
(a) Share of the overall mesophyll conductance limitation by the gas and liquid phases. (b) Components of the liquid phase limitation. Bars represent mean (±SE, n = 5–6) values.

analysis showed that g_s and g_m represent 20.0 and 22.2% of constraints, respectively. Moreover, as frequently observed in the literature (see Nadal & Flexas, 2019 and references therein), both g_s and g_m were tightly correlated with *A* across crop species (Figure 3). These results indicate that CO_2 diffusion conductance still has some space for photosynthesis improvement. The fact that good correlations between g_m_fluo and V_{cmax} and ETR were observed in the literature (Evans et al., 1994; Flexas et al., 2016) and in this study (Figure S3) suggests that a higher rate of CO_2 consumption requires an enhanced supply rate of CO_2 through increased g_m. The results support the statement in recent literature (see Gago et al., 2019 and references therein) that plant engineering efforts focusing on enhancing the catalytic rate of Rubisco alone are likely to be less effective in increasing photosynthetic productivity than parallel increases in both CO_2 supply and Rubisco activity. Moreover, increasing g_m is expected to improve crops' photosynthetic efficiency and intrinsic water use efficiency in parallel (Flexas et al., 2013, 2016).

Leaf anatomical traits cannot fully explain mesophyll conductance variation across C_3 crop species

Here, considerable variability in g_m between crops was observed, and it was correlated with *A* across crops (Figure 1). Although the photorespiratory CO_2 can service as an additional CO_2 source (Tholen et al., 2012), mesophyll conductance is usually considered as the efficiency of CO_2 movement from intercellular air spaces across the cell wall, plasma membrane, cytosol, chloroplast envelope, and stroma to Rubisco. In principle, each of these components inhibits CO_2 diffusion, and their CO_2 diffusion resistance values vary from species to species (Figure 6). As

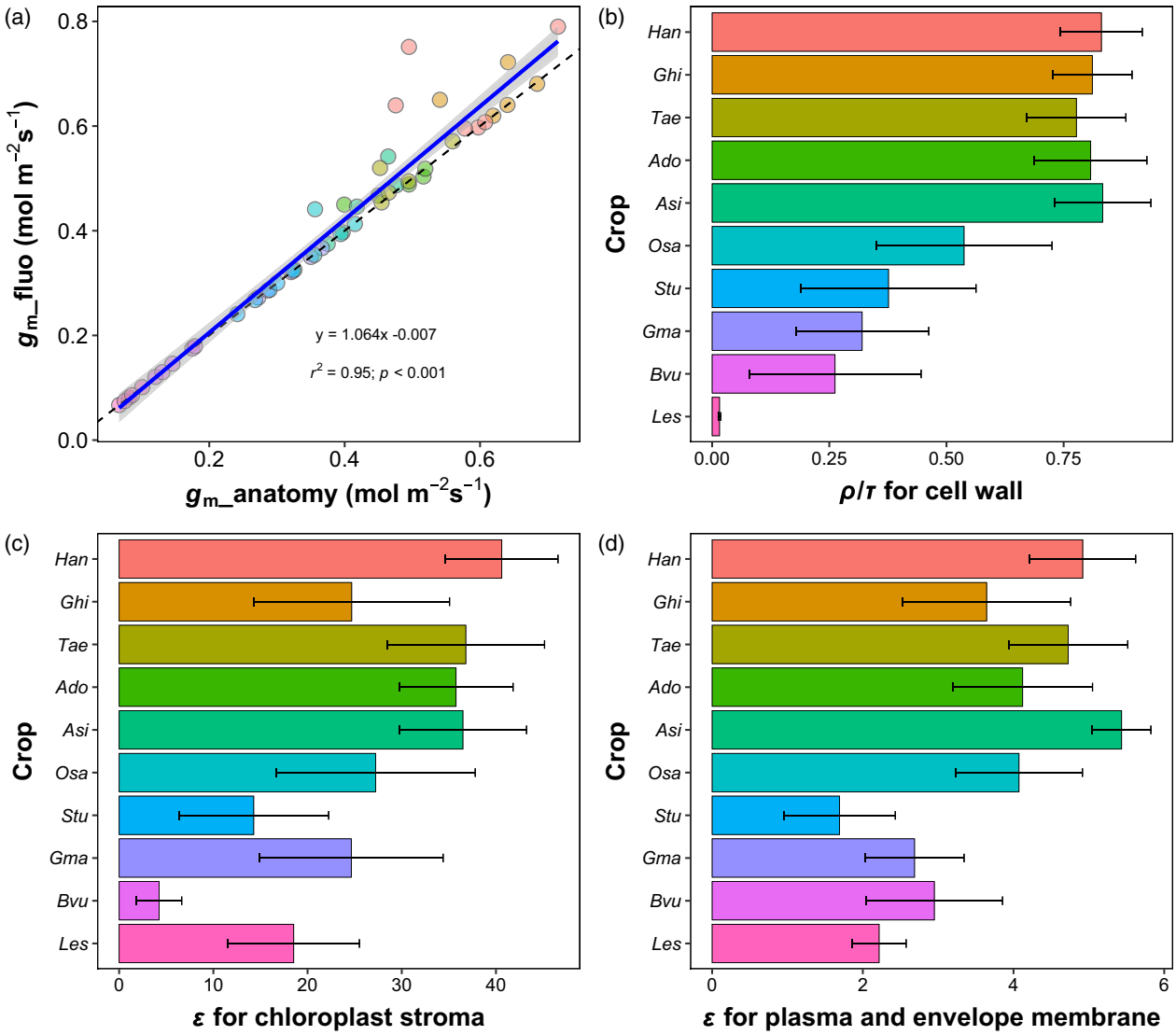

Figure 7. Estimations of cell wall effective porosity (ρ_i/τ_i) and facilitation effects (ε) for membranes and chloroplast stroma by minimizing the sum of squares between mesophyll diffusion conductance measured using the 'variable *J*' method (g_m_fluo) and modeled using leaf anatomical parameters (g_m_anatomy). (a) The relationship between g_m_fluo and the modeled g_m_anatomy by using species-dependent values of cell wall ρ_i/τ_i and the ε values of membranes and the chloroplast stroma. (b) Estimated ρ_i/τ_i for the cell wall. (c) Estimated ε for the chloroplast stroma. (d) Estimated ε for both plasma and envelope membranes. Blue lines represent the standardized major axis (SMA) regression lines, and the gray areas are 95% confidence intervals of the SMA regression lines. Bars represent mean (±SE, n = 5–6) values for each species.

mentioned in the introduction, leaf anatomical characteristics, especially cell wall thickness (T_{cw}) and the chloroplast surface facing intercellular air space (S_c), have been widely suggested to drive the variation in g_m across species. Unexpectedly, the observed variation of g_m across crops cannot be explained by the variation of T_{cw} or S_c. Further bicorrelation analysis between g_m_fluo and leaf anatomical traits showed that no leaf anatomical traits were correlated with g_m across species except chloroplast thickness (Figure 4). Although several studies claimed that CO_2 diffusion resistance in stroma could be low because its high pH and Rubisco concentrations could facilitate CO_2 diffusion (Mizokami et al., 2022; Terashima et al., 2011), here I observed that g_m was negatively correlated with stroma thickness, similar to other studies (Liu et al., 2021; Tosens, Niinemets, Vislap, et al., 2012; Veromann-Jürgenson et al., 2020). Clearly, more efforts are needed to reveal the impacts of stroma thickness on g_m.

In the present study, both S_c and T_{cw} were at the end of their spectrum (Figure S6; Flexas et al., 2021) with a narrow variability range, suggesting that those traits in crops might have been selected for during domestication

and/or evolution. Moreover, S_c is a 3D trait related to mesophyll cell and chloroplast shapes, and the estimation of S_c using two-dimensional (2D) images relied on broad assumptions. Recently, Harwood et al. (2020) along with other studies (Earles et al., 2018; Théroux-Rancourt et al., 2017) highlighted that the current techniques used to estimate 3D cell and chloroplast surface areas from 2D micrographs might contain uncertainty. In this sense, the lack of a significant relationship between g_m and S_c might be because of methodological errors. Unlike S_c, T_{cw} can be easily estimated using 2D images, although the measurement must be made where cell walls are perpendicular to the section.

The quantitative cellular limitation analysis indicated that the chloroplast stroma and cell wall were two major diffusion limitations in the liquid phase (Figure 6), and the g_m values estimated via the online carbon isotope and 'variable *J*' methods were much higher than the modeled values. Moreover, recent studies reported that the 1D anatomical model failed to catch the fast responses of g_m to light and nitrogen top-dress fertilization (Carriquí et al., 2019; Xiong & Flexas, 2021). Assuming the leaf anatomical measurements were accurate, the discarded results reflect other unmeasured traits that are essential to the CO_2 diffusion rate inside leaves. The effective porosity (ρ_i/τ_i) of cell walls was considered one of such unmeasured parameters (Evans, 2021; Evans et al., 2009). The ρ_i/τ_i value is set to a constant in the model (0.1 in the current study), but previous investigations suggested that it may vary significantly across species (see Evans, 2021 and references therein) and even for the same genotype grown in different light environments (Ellsworth et al., 2018). Here, the sensitivity analysis showed that a specific ρ_i/τ_i value for each species must be an input parameter to have the modeled g_m values matched to the g_m_fluo values if assuming the cell wall represents a major factor in liquid phase resistance (Figure S5). Differences in cell wall composition have been shown to impact ρ_i/τ_i (Carriquí et al., 2020; Ellsworth et al., 2018; Flexas et al., 2021).

Beyond anatomy, g_m is also regulated by biochemical features, such as aquaporin-mediated membrane permeability and CAs in the cytosol and stroma. However, the CO_2 diffusion conductance across the membranes and the aqueous phase diffusion coefficient in the cytosol and the chloroplast stroma were also set to constants in the model (Tomás et al., 2013; Tosens, Niinemets, Vislap, et al., 2012), and potential effects of facilitation were widely ignored (Mizokami et al., 2022). Although the enhancement factors (ε) due to facilitation processes of CO_2 transport in each element were not directly measured, the sensitivity analysis showed that the CO_2 diffusion conductance across membranes and the value of ε in the stroma could not be set as constant across species. For membranes, at least some aquaporins can facilitate CO_2 transportation across membranes (reviewed by Groszmann et al., 2017). In chloroplasts, the Rubisco protein tends to be distributed close to the cell wall, potentially decreasing the diffusion distance. Moreover, stromal CA is suggested to be the most abundant CA in C_3 plants, and the pH in the chloroplast under light is typically around 8.0. Therefore, the HCO_3^- concentration in the chloroplast stroma is much higher than in the cell wall and the cytosol, and the CO_2 diffusion conductance in chloroplasts could be enhanced significantly (Evans et al., 2009; Mizokami et al., 2022). Notably, although CAs also exist in the cytosol and the cytosol is slightly alkaline, the facilitation effects in the cytosol were not estimated in this study due to its minor limiting effects on liquid phase diffusion of CO_2.

As shown in Figure 7, the simulated cell wall effective porosity and facilitation effects for membranes and the chloroplast stroma varied dramatically among crops. As mentioned in previous studies (Evans, 2021; Tosens & Laanisto, 2018), whether large differences in those traits among species are real is an open question. Ellsworth et al. (2018) recently observed up to a 4-fold difference in the effective porosity of rice (*Oryza sativa*) mesophyll cell walls between plants grown at a photosynthetic photon flux density (PPFD) of 1000 or 300 μmol m^{-2} sec^{-1}. Their study also confirmed that different amounts of mixed linkage glucans in cell walls lead to differences in effective porosity between genotypes. Unfortunately, interspecies differences in the facilitation effects for membranes and chloroplast stroma have not been experimentally investigated. Therefore, further studies are required to better understand the mechanisms underlying the facilitation of CO_2 diffusion.

EXPERIMENTAL PROCEDURES

Plant materials

Arundo donax (Blossom), *Astragalus sinicus* (CW400), *Glycine max* (Ransom), *G. hirsutum* (Xinluzao), *H. annuus* (Russian Gigant), *L. esculentum* (a 'Tomàtiga de Ramellet' accession), *O. sativa* (Shanyou 63), *S. tuberosum* (Sifra), *B. vulgaris* (Detroit), and *Triticum aestivum* (Cajeme) were grown in a controlled environment growth chamber with a 12/12-h light/dark photoperiod, a PPFD at the pot height of 1000 μmol m^{-2} sec^{-1}, and an air temperature of 25°C during the day and 20°C during the night. Plants were grown in 5-L pots filled with commercial organic soil and perlite (4:1, v:v), and eight pots for each species were prepared. Plants were watered daily, and 100 ml Hoagland's solution was added to each pot weekly. Measurements were performed on 45–50-day-old plants. All measurements were performed on the youngest fully expanded leaf to ensure mature leaf anatomy and minimize leaf age variations among plants.

Gas exchange, chlorophyll fluorescence, and isotope measurements

An LI-6400XT photosynthesis system (LI-COR, Lincoln, NE, USA) equipped with a custom 8-cm^2 clear-topped chamber was used to

measure leaf gas exchange parameters. The block temperature, CO_2 concentration, flow rate, and relative air humidity inside the chamber were set at 25°C, 400 μmol mol^{-1}, 300 μmol sec^{-1}, and 70%, respectively. A stomatal ratio of 0.5 was used for all species. A 6400-18A RGB light source provided light, and the PPFD (white light) on the chamber surface was adjusted to 1500 μmol m^{-2} sec^{-1} during the acclimation stage (about 30 min). Then irradiance was changed to 100% red light for gas exchange and chlorophyll fluorescence measurements. The subsamples of gas from the reference line (between the console and the CO_2 gas cylinders used in the LI-6400XT CO_2 injector system) and the sample line (chamber exhaust) of the LI-6400XT system were connected to a stable carbon isotope tunable diode laser (TDL, TGA100A; Campbell Scientific, Logan UT, USA) through 'T' junction tubes (for more details, see Douthe et al., 2011). The TDL system was carefully calibrated following the protocol provided by Douthe et al. (2011). The leaf chlorophyll fluorescence parameters were also measured using a pulse-modulated chlorophyll fluorescence meter (Junior PAM, Walz, Germany) once the LI-COR 6400XT recorded the gas exchange parameters. The time lag between the LI-COR 6400XT and the Junior PAM was assumed to be zero. The TDL and gas exchange data were matched by taking an average time lag of 42 sec. For each species, at least five individuals were investigated.

The actual photochemical efficiency of photosystem II (Φ_{PSII}) and ETR were calculated as follows:

$$\Phi_{PSII} = \frac{F'_m - F_s}{F'_m},$$

$$ETR = \Phi_{PSII} \cdot PPFD \cdot \alpha\beta,$$

where the F_s is the steady-state fluorescence, F'_m is the maximum fluorescence, α is the leaf absorbance, and β is the partitioning of absorbed quanta between photosystems II and I. The value of α (Table S1) was estimated using a spectroradiometer (HR2000CG-UV-NIR; Ocean Optics, Inc., Dunedin, FL, USA), and the value of β was assumed to be 0.5 (Carriquí et al., 2015).

The chlorophyll fluorescence-based 'variable *J*' method (Harley et al., 1992) was used to calculate the mesophyll conductance ($g_{m_}$fluo) as follows:

$$g_{m\_}fluo = \frac{A}{C_i - \frac{\Gamma^* \cdot (ETR + 8 \cdot (A + R_d))}{ETR - 4 \cdot (A + R_d)}},$$

where A is the photosynthetic rate, C_i is the intercellular CO_2 concentration, and Γ* is the CO_2 compensation point in the absence of respiration. The values of A and C_i were directly taken from the gas exchange measurements. The value of Γ* can be estimated using the ambient O_2 concentration (O, 210 000 μmol mol^{-1}) and the Rubisco specificity factor ($S_{c/o}$; $\Gamma^* = 0.5\ O/S_{c/o}$) of the species (Galmés et al., 2017). The $S_{c/o}$ values of most C_3 crop species were investigated by Hermida-Carrera et al. (2016). Although the temperature responses of $S_{c/o}$ varied dramatically among species, the $S_{c/o}$ values of C_3 crops at 25°C were quite similar. Therefore, a typical $S_{c/o}$ value of 97.5 mol mol^{-1} at 25°C was selected for all the species in the present study. R_d is the daytime respiration rate, which was assumed to be half of the dark respiration rate (Niinemets et al., 2005). The dark respiration measurements were conducted in dark-adapted leaves using an LI-6400XT system equipped with a 6400-02B leaf chamber.

Isotopic discrimination ($\Delta^{13}C$) by leaves was evaluated by the carbon isotope composition difference of the sample line and the reference line (Evans et al., 1986). The ^{13}C-based mesophyll conductance ($g_{m\_}\Delta^{13}C$) was estimated by combining gas exchange parameters and isotopic discrimination (Barbour et al., 2010; Douthe et al., 2011; Evans et al., 1986). Farquhar and Cernusak (2012) highlight the impacts of the ternary effect on mesophyll conductance estimation; therefore, the ternary corrections were included in the $g_{m\_}\Delta^{13}C$ calculation. By assuming an infinite mesophyll conductance, the ^{13}C discrimination ($\Delta^{13}C$) can be calculated as follows (Barbour, Evans, et al., 2016):

$$\Delta^{13}C = \frac{1}{1-t}\left[a_b\frac{C_a - C_s}{C_a} + a_s\frac{C_s - C_i}{C_a}\right] + \frac{1+t}{1-t}\left[b\frac{C_i}{C_a} - \frac{\alpha_b}{\alpha_{e'}}\cdot e'\cdot\frac{R_d}{A+R_d}\cdot\frac{C_i - \Gamma^*}{C_a} - \frac{\alpha_b}{\alpha_f}\cdot f\cdot\frac{\Gamma^*}{C_a}\right],$$

$$t = \frac{(1+a')E}{2g_{ac}},$$

$$a' = \frac{a_b(C_a - C_s) + a_b(C_s - C_i)}{C_a - C_i},$$

where C_a and C_s are the ambient and leaf surface CO_2 concentration, respectively, E is the transpiration rate, a_b, a_s, b, f, and e' are the fractionations associated with the boundary layer (2.9‰), the stomatal pores (4.4‰), carboxylation (29‰), photorespiration (16.2‰), and day respiration (20.5‰), respectively, α_b, $\alpha_{e'}$, and α_f are fractionation factors for carboxylation ($1 + b$), day respiration ($1 + e'$), and photorespiration ($1 + f$), respectively, t is the ternary correlation factor, E is the transpiration rate, a' is the combined fractionation factor to CO_2 diffusion through the leaf boundary layer and stomata, and g_{ac} is the total CO_2 diffusion conductance through the leaf boundary layer and stomata.

The difference between $\Delta^{13}C$ and the observed ^{13}C discrimination ($\Delta^{13}C_{obs}$) is mainly caused by the mesophyll diffusion conductance. The value of $g_{m\_}\Delta^{13}C$ was estimated as follows:

$$g_{m\_}\Delta^{13}C = \frac{A\left(b - a_m - \frac{\alpha_b}{\alpha_{e'}}\cdot e'\cdot\frac{R_d}{A+R_d}\right)}{\frac{1-t}{1+t}\cdot\left(\Delta^{13}C - \Delta^{13}C_{obs}\right)\cdot C_a},$$

where a_m is the fractionation during diffusion and dissolution of CO_2 (0.7‰).

Photosynthetic limitation analysis

In the current study, the relative photosynthetic limitations were analyzed following the method described in Grassi and Magnani (2005). In this approach, the total photosynthetic limitation is divided into the relative limitations of stomata (l_s), mesophyll (l_m), and biochemistry (l_b):

$$l_s = \frac{g_t/g_s \cdot \partial A/\partial C_c}{g_t + \partial A/\partial C_c},$$

$$l_m = \frac{g_t/g_m \cdot \partial A/\partial C_c}{g_t + \partial A/\partial C_c},$$

$$l_b = \frac{g_t}{g_t + \partial A/\partial C_c},$$

where g_t is the total conductance:

$$g_t = \frac{1}{1/g_s + 1/g_m}.$$

In the present study, the $g_{m_}$fluo values were used in the relative limitation analysis. The ratio $\partial A/\partial C_c$ is the slope of the A

versus C_c curve. Based on the FvCB model equations (Farquhar et al., 1980), $\partial A/\partial C_c$ can be expressed as follows:

$$\partial A/\partial C_c = V_{cmax} \cdot \frac{\Gamma^* + K_m}{(C_c + K_m)^2}.$$

The 'one-point' method (de Kauwe et al., 2016) was used to calculate the maximum carboxylation capacity (V_{cmax}) as follows:

$$V_{cmax} = A\left(\frac{C_i + K_m}{C_i - \Gamma^*} - 0.015\right),$$

$$K_m = k_c \cdot \left(\frac{O_i}{k_o} + 1\right),$$

where K_m is the Michaelis–Menten constant, k_c is the Michaelis constant for carboxylation, k_o is the Michaelis constant for oxygenation, and O_i is the oxygen content in the intercellular air space. I chiefly used k_c and k_o values reported by Bernacchi et al. (2002).

Leaf anatomical measurements

After the gas exchange measurements, leaves were sampled for leaf anatomical estimation. Three subsamples were taken from the top, middle, and bottom of each leaf. For each species, five or six individual plants were sampled. The leaf anatomical measurements were made as described in Xiong and Flexas (2021). The intercellular air space fraction (f_{iAS}), mesophyll cell wall thickness (T_{cw}), mesophyll cell surface area facing the intercellular air space (S_m), and chloroplast surface area facing the intercellular air space (S_c) were measured and/or calculated based on the light and transmission electron microscopy images (Figure S1; see details in Xiong & Flexas, 2021). At least 10 light or transmission microscopy slices were evaluated for each leaf. More than 50 light or transmission microscopy slices were analyzed for each species to produce reliable anatomical parameters (Harwood et al., 2020; Théroux-Rancourt et al., 2017). Thain (1983) curvature correction factors (Table S1) of palisade ($F_{palisade}$) and spongy (F_{spongy}) cells were calculated using the R script provided in Théroux-Rancourt et al. (2017).

Mesophyll conductance modeled from anatomical characteristics

To evaluate the influences of anatomical traits on the mesophyll conductance variation among species (Carriquí et al., 2019; Tomás et al., 2013; Tosens, Niinemets, Westoby, et al., 2012), the anatomy-based mesophyll conductance ($g_{m\_anatomy}$) was modeled following the equations originally developed by Niinemets and Reichstein (2003) and modified parameters presented by Evans et al. (2009) were applied to provide an anatomy-based estimate of $g_{m\_anatomy}$. First, $g_{m\_anatomy}$ was divided into (i) a gas phase conductance between the substomatal cavities and the outer surface of cell walls (g_{ias}) and (ii) a liquid phase conductance between the outer surface of the cell walls and the site of carboxylation in the chloroplast stroma (g_{liq}):

$$g_{manatomy} = \frac{1}{\frac{1}{g_{ias}} + \frac{RT}{H \cdot g_{liq}}},$$

where R is the gas constant, T is the absolute temperature, and H is the Henry constant.

The value of g_{ias} was calculated based on f_{ias} and the diffusion path length in the gas phase, which is assumed to be half of the mesophyll thickness (T_{mes}):

$$g_{ias} = \frac{D_{air} \cdot f_{ias}}{\frac{1}{2} T_{mes} \cdot \varsigma},$$

where D_a is the diffusion coefficient for CO_2 in the gas phase (1.51×10^{-5} m^2 sec^{-1} at 25°C) and ς is the diffusion path tortuosity, which is fixed at 1.57 m m^{-1} as in previous studies mentioned above.

The value of g_{liq} was calculated as follows:

$$g_{liq} = \frac{1}{\sum \frac{1}{g_i}} \cdot S_c,$$

where g_i is the conductance of the cell wall, plasmalemma, cytosol, chloroplast envelope, or chloroplast stroma. The conductance of a given component of the diffusion pathway was calculated as follows:

$$g_i = \frac{\rho_i \cdot D \cdot \gamma_i}{\tau_i \cdot \Delta L_i},$$

where D is the aqueous phase diffusion coefficient for CO_2, ρ_i is the porosity of the element, γ_i accounts for the decrease of diffusion conductance compared with free diffusion in water, τ_i is the tortuosity of the pathway through the element, and ΔL_i is the diffusion path length, which is usually the thickness of a component, or half the thickness of the chloroplast when calculating stroma conductance. To reduce the number of unknown parameters, the porosity was combined with tortuosity into a single term (ρ_i/τ_i), the effective porosity (Evans et al., 2009). Because the structural parameters of the plasma membrane and chloroplast envelope are impossible to estimate from light or electron microscopy images, an estimated value of 0.0035 m sec^{-1} for both plasma membrane conductance (g_{pl}) and chloroplast envelope conductance (g_{en}) (halved to account for it being two membranes) was used as in previous studies (Carriquí et al., 2019; Niinemets & Reichstein, 2003; Tomás et al., 2013; Tosens, Niinemets, Vislap, et al., 2012). Following the calculations in Tosens, Niinemets, Vislap, et al. (2012), the values of the parameters selected for calculating mesophyll conductance are shown in Table S2.

Quantitative analysis of anatomical constraints

The relative limitation of gas phase conductance (l_{ias}) to mesophyll conductance was calculated as follows:

$$l_{ias} = \frac{g_{m\_anatomy}}{g_{ias}}.$$

The relative limitation of different components of the liquid phase conductance (l_i) was calculated as follows:

$$l_i = \frac{g_{m\_anatomy}}{g_i \cdot S_c},$$

where g_i refers to the diffusion conductance in each cellular component (e.g., cell wall, plasma membrane, cytosol, chloroplast envelope, and chloroplast stroma) introduced above and the l_i is the component limitation.

Estimation of the effective porosity and facilitation effects

As discussed in many recent studies (Evans, 2021; Evans et al., 2009; Mizokami et al., 2022), the CO_2 diffusion conductance can be potentially enhanced by many other factors, such as specific protein channels in membranes, fast conversion of CO_2 to bicarbonate catalyzed by CAs in the cytosol and stroma, and concentrated Rubisco in the stroma. Therefore, the term that accounts

for the effect of facilitation of CO_2 transport in each component can be expressed as follows:

$$g_i = \frac{\rho_i \cdot D \cdot \gamma_i}{\tau_i \cdot \Delta L_i} \cdot (1 + \epsilon_i),$$

where ε_i is defined as the enhancement due to facilitation processes in that component (Evans et al., 2009); ε was rarely considered in previous studies because of difficulties in the estimation of those values. In this study, I estimated the values of ε for stroma and membranes using the *Solver* function (via the least squares method) in Microsoft Excel (Microsoft Corporation; Redmond, WA, USA) along with the ρ_i/τ_i values of cell walls for each species by minimizing the mean squared error between $g_{m_}$fluo and $g_{m_}$anatomy values. In this analysis, the ε values for stroma and membranes were set to vary between 0 and 50 (Mizokami et al., 2022) and between 0 and 6 (Evans et al., 2009), respectively. The ρ_i/τ_i values for the cell wall were set to vary between 0 and 0.96 (Ellsworth et al., 2018).

Statistical analysis

One-way analysis of variance (ANOVA) was used to test the differences in measured traits among species, and Tukey's test was adopted to make pairwise comparisons at the 0.05 level using the *multcomp* package. The standardized major axis (SMA) analysis was performed to test the correlations between traits using the *smart* package. The one-sample test was conducted to test if the slope and the intercept of the $g_{m_}$fluo versus $g_{m\_}\Delta^{13}C$ SMA regression differ from 1 and 0, respectively. Statistical analyses were conducted and results were visualized using R version 4.2.2 (R Core Team, 2022).

AUTHOR CONTRIBUTIONS

DX designed the research, performed the experiment, analyzed the data, and wrote the manuscript.

ACKNOWLEDGMENTS

I was supported by the National Natural Science Foundation of China (No. 32022060) and the China Agriculture Research System (CARS-01-23).

CONFLICT OF INTEREST

The author declares no conflict of interest.

DATA AVAILABILITY STATEMENT

All relevant data can be found within the article and its supporting materials.

SUPPORTING INFORMATION

Additional Supporting Information may be found in the online version of this article.

Figure S1. Graphical representation of the different variables measured on two-dimensional sections.

Figure S2. Representative leaf cross-section micrograph for each species.

Figure S3. Variation of photosynthetic capacity across crop species.

Figure S4. Leaf anatomical characteristics of crop species.

Figure S5. Correlations of mesophyll conductance and leaf anatomical traits.

Figure S6. Relationships between mesophyll conductance and cell structural traits from the present study and the global dataset of Flexas et al. (2021).

Table S1. Leaf absorbance and Thain's curvature correction factor for palisade and spongy mesophyll cells.

Table S2. Selected input parameters in the one-dimensional anatomical mesophyll conductance model.

Table S3. One-way ANOVA results for the differences in photosynthetic and anatomical traits between species.

REFERENCES

Barbour, M.M. (2017) Understanding regulation of leaf internal carbon and water transport using online stable isotope techniques. *The New Phytologist*, **213**, 83–88.

Barbour, M.M., Bachmann, S., Bansal, U., Bariana, H. & Sharp, P. (2016) Genetic control of mesophyll conductance in common wheat. *The New Phytologist*, **209**, 461–465.

Barbour, M.M., Evans, J.R., Simonin, K.A. & von Caemmerer, S. (2016) Online CO_2 and H_2O oxygen isotope fractionation allows estimation of mesophyll conductance in C_4 plants, and reveals that mesophyll conductance decreases as leaves age in both C_4 and C_3 plants. *The New Phytologist*, **210**, 875–889.

Barbour, M.M. & Kaiser, B.N. (2016) The response of mesophyll conductance to nitrogen and water availability differs between wheat genotypes. *Plant Science*, **251**, 119–127.

Barbour, M.M., Warren, C.R., Farquhar, G.D., Forrester, G. & Brown, H. (2010) Variability in mesophyll conductance between barley genotypes, and effects on transpiration efficiency and carbon isotope discrimination. *Plant, Cell & Environment*, **33**, 1176–1185.

Bernacchi, C.J., Portis, A.R., Nakano, H., von Caemmerer, S. & Long, S.P. (2002) Temperature response of mesophyll conductance. Implications for the determination of rubisco enzyme kinetics and for limitations to photosynthesis *in vivo*. *Plant Physiology*, **130**, 1992–1998.

Borsuk, A.M., Roddy, A.B., Théroux-Rancourt, G. & Brodersen, C.R. (2022) Structural organization of the spongy mesophyll. *The New Phytologist.*, **234**, 946–960. Available from: https://doi.org/10.1111/nph.17971

Cano, F.J., López, R. & Warren, C.R. (2014) Implications of the mesophyll conductance to CO_2 for photosynthesis and water-use efficiency during long-term water stress and recovery in two contrasting *Eucalyptus* species. *Plant, Cell and Environment*, **37**, 2470–2490.

Carriquí, M., Cabrera, H.M., Conesa, M.À., Coopman, R.E., Douthe, C., Gago, J. *et al.* (2015) Diffusional limitations explain the lower photosynthetic capacity of ferns as compared with angiosperms in a common garden study. *Plant, Cell & Environment*, **38**, 448–460.

Carriquí, M., Douthe, C., Molins, A. & Flexas, J. (2019) Leaf anatomy does not explain apparent short-term responses of mesophyll conductance to light and CO_2 in tobacco. *Physiologia Plantarum*, **165**, 604–618.

Carriquí, M., Nadal, M., Clemente-Moreno, M.J., Gago, J., Miedes, E. & Flexas, J. (2020) Cell wall composition strongly influences mesophyll conductance in gymnosperms. *The Plant Journal*, **103**, 1372–1385.

Clarke, V.C., Danila, F.R. & von Caemmerer, S. (2021) CO_2 diffusion in tobacco: a link between mesophyll conductance and leaf anatomy. *Interface focus*, **11**, 20200040.

Clemente-Moreno, M.J., Gago, J., Díaz-Vivancos, P., Bernal, A., Miedes, E., Bresta, P. *et al.* (2019) The apoplastic antioxidant system and altered cell wall dynamics influence mesophyll conductance and the rate of photosynthesis. *The Plant Journal*, **99**, 1031–1046.

Cousins, A.B., Mullendore, D.L. & Sonawane, B.V. (2020) Recent developments in mesophyll conductance in C3, C4, and crassulacean acid metabolism plants. *The Plant Journal*, **101**, 816–830.

de Kauwe, M.G., Lin, Y.-S., Wright, I.J., Medlyn, B.E., Crous, K.Y., Ellsworth, D.S. *et al.* (2016) A test of the 'one-point method' for estimating maximum carboxylation capacity from field-measured, light-saturated photosynthesis. *The New Phytologist*, **210**, 1130–1144.

Douthe, C., Dreyer, E., Epron, D. & Warren, C.R. (2011) Mesophyll conductance to CO_2, assessed from online TDL-AS records of $^{13}CO_2$ discrimination, displays small but significant short-term responses to CO and irradiance in *Eucalyptus* seedlings. *Journal of Experimental Botany*, **62**, 5335–5346.

Earles, J.M., Théroux-Rancourt, G., Roddy, A.B., Gilbert, M.E., McElrone, A.J. & Brodersen, C.R. (2018) Beyond porosity: 3D leaf intercellular airspace traits that impact mesophyll conductance. *Plant Physiology*, **178**, 148–162.

Elferjani, R., Benomar, L., Momayyezi, M., Tognetti, R., Niinemets, Ü., Soolanayakanahally, R.Y. *et al.* (2021) A meta-analysis of mesophyll conductance to CO_2 in relation to major abiotic stresses in poplar species. *Journal of Experimental Botany*, **72**, 4384–4400.

Ellsworth, P.V., Ellsworth, P.Z., Koteyeva, N.K. & Cousins, A.B. (2018) Cell wall properties in *Oryza sativa* influence mesophyll CO_2 conductance. *The New Phytologist*, **219**, 66–76.

Ethier, G.J. & Livingston, N.J. (2004) On the need to incorporate sensitivity to CO_2 transfer conductance into the Farquhar-von Caemmerer-Berry leaf photosynthesis model. *Plant, Cell & Environment*, **27**, 137–153.

Evans, J.R. (1999) Leaf anatomy enables more equal access to light and CO_2 between chloroplasts. *The New Phytologist*, **143**, 93–104.

Evans, J.R. (2021) Mesophyll conductance: walls, membranes and spatial complexity. *The New Phytologist*, **229**, 1864–1876.

Evans, J.R., Kaldenhoff, R., Genty, B. & Terashima, I. (2009) Resistances along the CO_2 diffusion pathway inside leaves. *Journal of Experimental Botany*, **60**, 2235–2248.

Evans, J.R., Sharkey, T.D., Berry, J.A. & Farquhar, G.D. (1986) Carbon isotope discrimination measured concurrently with gas exchange to investigate CO_2 diffusion in leaves of higher plants. *Functional Plant Biology*, **13**, 281.

Evans, J.R. & von Caemmerer, S. (1996) Carbon dioxide diffusion inside leaves. *Plant Physiology*, **110**, 339–346.

Evans, J.R., von Caemmerer, S., Setchell, B.A. & Hudson, G.S. (1994) The relationship between CO_2 transfer conductance and leaf anatomy in transgenic tobacco with a reduced content of rubisco. *Functional Plant Biology*, **21**, 475.

Farquhar, G.D. & Cernusak, L.A. (2012) Ternary effects on the gas exchange of isotopologues of carbon dioxide. *Plant, Cell & Environment*, **35**, 1221–1231.

Farquhar, G.D., von Caemmerer, S. & Berry, J.A. (1980) A biochemical model of photosynthetic CO_2 assimilation in leaves of C_3 species. *Planta*, **149**, 78–90.

Flexas, J., Barbour, M.M., Brendel, O., Cabrera, H.M., Carriquí, M., Díaz-Espejo, A. *et al.* (2012) Mesophyll diffusion conductance to CO_2: an unappreciated central player in photosynthesis. *Plant Science*, **193**(194), 70–84.

Flexas, J., Cano, F.J., Carriquí, M., Coopman, R.E., Mizokami, Y., Tholen, D. *et al.* (2018) CO_2 diffusion inside photosynthetic organs. In: Adams, W.W., III & Terashima, I. (Eds.) *The leaf: a platform for performing photosynthesis*. Cham: Springer International Publishing, pp. 163–208.

Flexas, J., Clemente-Moreno, M.J., Bota, J., Brodribb, T.J., Gago, J., Mizokami, Y. *et al.* (2021) Cell wall thickness and composition are involved in photosynthetic limitation. *Journal of Experimental Botany*, **72**, 3971–3986.

Flexas, J., Díaz-Espejo, A., Conesa, M.A., Coopman, R.E., Douthe, C., Gago, J. *et al.* (2016) Mesophyll conductance to CO_2 and rubisco as targets for improving intrinsic water use efficiency in C_3 plants. *Plant, Cell & Environment*, **39**, 965–982.

Flexas, J., Niinemets, Ü., Gallé, A., Barbour, M.M., Centritto, M., Díaz-Espejo, A. *et al.* (2013) Diffusional conductances to CO_2 as a target for increasing photosynthesis and photosynthetic water-use efficiency. *Photosynthesis Research*, **117**, 45–59.

Gago, J., Carriquí, M., Nadal, M., Clemente-Moreno, M.J., Coopman, R.E., Fernie, A.R. *et al.* (2019) Photosynthesis optimized across land plant phylogeny. *Trends in Plant Science*, **24**, 947–958.

Galmés, J., Molins, A., Flexas, J. & Conesa, M.À. (2017) Coordination between leaf CO_2 diffusion and rubisco properties allows maximizing photosynthetic efficiency in *Limonium* species. *Plant, Cell & Environment*, **40**, 2081–2094.

Grassi, G. & Magnani, F. (2005) Stomatal, mesophyll conductance and biochemical limitations to photosynthesis as affected by drought and leaf ontogeny in ash and oak trees. *Plant, Cell and Environment*, **28**, 834–849.

Griffiths, H. & Helliker, B.R. (2013) Mesophyll conductance: internal insights of leaf carbon exchange. *Plant, Cell & Environment*, **36**, 733–735.

Groszmann, M., Osborn, H.L. & Evans, J.R. (2017) Carbon dioxide and water transport through plant aquaporins. *Plant, Cell and Environment*, **40**, 938–961.

Gu, L. & Sun, Y. (2014) Artefactual responses of mesophyll conductance to CO_2 and irradiance estimated with the variable J and online isotope discrimination methods. *Plant, Cell & Environment*, **37**, 1231–1249.

Harley, P.C., Loreto, F., Di Marco, G. & Sharkey, T.D. (1992) Theoretical considerations when estimating the mesophyll conductance to CO_2 flux by analysis of the response of photosynthesis to CO_2. *Plant Physiology*, **98**, 1429–1436.

Harwood, R., Goodman, E., Gudmundsdottir, M., Huynh, M., Musulin, Q., Song, M. *et al.* (2020) Cell and chloroplast anatomical features are poorly estimated from 2D cross-sections. *The New Phytologist*, **225**, 2567–2578.

Hermida-Carrera, C., Kapralov, M.V. & Galmés, J. (2016) Rubisco catalytic properties and temperature response in crops. *Plant Physiology*, **171**, 2549–2561.

Huang, X., Wang, Z., Huang, J., Peng, S. & Xiong, D. (2021) Mesophyll conductance variability of rice aquaporin knockout lines at different growth stages and growing environments. *The Plant Journal*, **107**, 1503–1512.

Liu, M., Liu, X., Du, X., Korpelainen, H., Niinemets, Ü. & Li, C. (2021) Anatomical variation of mesophyll conductance due to salt stress in *Populus cathayana* females and males growing under different inorganic nitrogen sources. *Tree Physiology*, **41**, 1462–1478.

Lloyd, J., Syvertsen, J.P., Kriedemann, P.E. & Farquhar, G.D. (1992) Low conductances for CO_2 diffusion from stomata to the sites of carboxylation in leaves of woody species. *Plant, Cell & Environment*, **15**, 873–899.

Long, S.P., Zhu, X.-G., Naidu, S.L. & Ort, D.R. (2006) Can improvement in photosynthesis increase crop yields? *Plant, Cell & Environment*, **29**, 315–330.

Lundgren, M.R. & Fleming, A.J. (2020) Cellular perspectives for improving mesophyll conductance. *The Plant Journal*, **101**, 845–857.

Milla, R., Osborne, C.P., Turcotte, M.M. & Violle, C. (2015) Plant domestication through an ecological lens. *Trends in Ecology & Evolution*, **30**, 463–469.

Mizokami, Y., Oguchi, R., Sugiura, D., Yamori, W., Noguchi, K. & Terashima, I. (2022) Cost-benefit analysis of mesophyll conductance: diversities of anatomical, biochemical and environmental determinants. *Annals of Botany*, **130**, 265–283.

Mizokami, Y., Sugiura, D., Watanabe, C.K.A., Betsuyaku, E., Inada, N. & Terashima, I. (2019) Elevated CO_2-induced changes in mesophyll conductance and anatomical traits in wild type and carbohydrate-metabolism mutants of Arabidopsis. *Journal of Experimental Botany*, **70**, 4807–4818.

Nadal, M. & Flexas, J. (2019) Variation in photosynthetic characteristics with growth form in a water-limited scenario: implications for assimilation rates and water use efficiency in crops. *Agricultural Water Management*, **216**, 457–472.

Niinemets, Ü., Díaz-Espejo, A., Flexas, J., Galmés, J. & Warren, C.R. (2009) Role of mesophyll diffusion conductance in constraining potential photosynthetic productivity in the field. *Journal of Experimental Botany*, **60**, 2249–2270.

Niinemets, Ü. & Reichstein, M. (2003) Controls on the emission of plant volatiles through stomata: differential sensitivity of emission rates to stomatal closure explained. *Journal of Geophysical Research*, **108**(D7), 4208. https://doi.org/10.1029/2002JD002620

Niinemets, Ü., Wright, I.J. & Evans, J.R. (2009) Leaf mesophyll diffusion conductance in 35 Australian sclerophylls covering a broad range of foliage structural and physiological variation. *Journal of Experimental Botany*, **60**, 2433–2449.

Niinemets, U.L., Cescatti, A., Rodeghiero, M. & Tosens, T. (2005) Leaf internal diffusion conductance limits photosynthesis more strongly in older leaves of Mediterranean evergreen broad-leaved species. *Plant, Cell & Environment*, **28**, 1552–1566.

Onoda, Y., Wright, I.J., Evans, J.R., Hikosaka, K., Kitajima, K., Niinemets, Ü. *et al.* (2017) Physiological and structural tradeoffs underlying the leaf economics spectrum. *The New Phytologist*, **214**, 1447–1463.

Pons, T.L., Flexas, J., von Caemmerer, S., Evans, J.R., Genty, B., Ribas-Carbó, M. *et al.* (2009) Estimating mesophyll conductance to CO_2: methodology, potential errors, and recommendations. *Journal of Experimental Botany*, **60**, 2217–2234.

R Core Team. (2022) *R: A language and environment for statistical computing*. Vienna, Austria: R Foundation for Statistical Computing. https://www.R-project.org/

Roig-Oliver, M., Bresta, P., Nadal, M., Liakopoulos, G., Nikolopoulos, D., Karabourniotis, G. *et al.* (2020) Cell wall composition and thickness affect mesophyll conductance to CO_2 diffusion in *Helianthus annuus* under water deprivation. *Journal of Experimental Botany*, **71**, 7198–7209.

Sharkey, T.D., Bernacchi, C.J., Farquhar, G.D. & Singsaas, E.L. (2007) Fitting photosynthetic carbon dioxide response curves for C_3 leaves. *Plant, Cell & Environment*, **30**, 1035–1040.

Sonawane, B.V., Koteyeva, N.K., Johnson, D.M. & Cousins, A.B. (2021) Differences in leaf anatomy determines temperature response of leaf hydraulic and mesophyll CO_2 conductance in phylogenetically related C_4 and C_3 grass species. *The New Phytologist*, **230**, 1802–1814.

Sugiura, D., Terashima, I. & Evans, J.R. (2020) A decrease in mesophyll conductance by cell-wall thickening contributes to photosynthetic downregulation. *Plant Physiology*, **183**, 1600–1611.

Terashima, I., Hanba, Y.T., Tholen, D. & Niinemets, Ü. (2011) Leaf functional anatomy in relation to photosynthesis. *Plant Physiology*, **155**, 108–116.

Thain, J.F. (1983) Curvature correction factors in the measurement of cell surface areas in plant tissues. *Journal of Experimental Botany*, **34**, 87–94.

Théroux-Rancourt, G., Earles, J.M., Gilbert, M.E., Zwieniecki, M.A., Boyce, C.K., McElrone, A.J. *et al.* (2017) The bias of a two-dimensional view: comparing two-dimensional and three-dimensional mesophyll surface area estimates using noninvasive imaging. *The New Phytologist*, **215**, 1609–1622.

Théroux-Rancourt, G. & Gilbert, M.E. (2017) The light response of mesophyll conductance is controlled by structure across leaf profiles. *Plant, Cell & Environment*, **40**, 726–740.

Tholen, D., Ethier, G., Genty, B., Pepin, S. & Zhu, X.-G. (2012) Variable mesophyll conductance revisited: theoretical background and experimental implications. *Plant, Cell and Environment*, **35**, 2087–2103.

Tomás, M., Flexas, J., Copolovici, L., Galmés, J., Hallik, L., Medrano, H. *et al.* (2013) Importance of leaf anatomy in determining mesophyll diffusion conductance to CO_2 across species: quantitative limitations and scaling up by models. *Journal of Experimental Botany*, **64**, 2269–2281.

Tosens, T. & Laanisto, L. (2018) Mesophyll conductance and accurate photosynthetic carbon gain calculations. *Journal of Experimental Botany*, **69**, 5315–5318.

Tosens, T., Niinemets, Ü., Vislap, V., Eichelmann, H. & Castro, D.P. (2012) Developmental changes in mesophyll diffusion conductance and photosynthetic capacity under different light and water availabilities in *Populus tremula*: how structure constrains function. *Plant, Cell & Environment*, **35**, 839–856.

Tosens, T., Niinemets, Ü., Westoby, M. & Wright, I.J. (2012) Anatomical basis of variation in mesophyll resistance in eastern Australian sclerophylls: news of a long and winding path. *Journal of Experimental Botany*, **63**, 5105–5119.

Veromann-Jürgenson, L.-L., Brodribb, T.J., Niinemets, Ü. & Tosens, T. (2020) Variability in the chloroplast area lining the intercellular airspace and cell walls drives mesophyll conductance in gymnosperms. *Journal of Experimental Botany*, **71**, 4958–4971.

von Caemmerer, S. (2000) *Biochemical models of leaf photosynthesis*. Victoria, Australia: CSIRO Publishing. Available at: https://doi.org/10.1071/9780643103405

von Caemmerer, S. & Evans, J.R. (2015) Temperature responses of mesophyll conductance differ greatly between species. *Plant, Cell & Environment*, **38**, 629–637.

von Caemmerer, S. & Farquhar, G.D. (1981) Some relationships between the biochemistry of photosynthesis and the gas exchange of leaves. *Planta*, **153**, 376–387.

Wang, X., Du, T., Huang, J., Peng, S. & Xiong, D. (2018) Leaf hydraulic vulnerability triggers the decline in stomatal and mesophyll conductance during drought in rice. *Journal of Experimental Botany*, **69**, 4033–4045.

Xiong, D., Douthe, C. & Flexas, J. (2018) Differential coordination of stomatal conductance, mesophyll conductance, and leaf hydraulic conductance in response to changing light across species. *Plant, Cell & Environment*, **41**, 436–450.

Xiong, D. & Flexas, J. (2021) Leaf anatomical characteristics are less important than leaf biochemical properties in determining photosynthesis responses to nitrogen top-dressing. *Journal of Experimental Botany*, **72**, 5709–5720.

Xiong, D., Flexas, J., Huang, J., Cui, K., Wang, F., Douthe, C. *et al.* (2022) Why high yield QTLs failed in preventing yield stagnation in rice? *Crop and Environment*, **1**, 103–107.

Xiong, D., Flexas, J., Yu, T., Peng, S. & Huang, J. (2017) Leaf anatomy mediates coordination of leaf hydraulic conductance and mesophyll conductance to CO_2 in *Oryza*. *The New Phytologist*, **213**, 572–583.

Xiong, D., Liu, X., Liu, L., Douthe, C., Li, Y., Peng, S. *et al.* (2015) Rapid responses of mesophyll conductance to changes of CO_2 concentration, temperature and irradiance are affected by N supplements in rice. *Plant, Cell & Environment*, **38**, 2541–2550.

Zhu, X.-G., Hasanuzzaman, M., Jajoo, A., Lawson, T., Lin, R., Liu, C.-M. *et al.* (2022) Improving photosynthesis through multidisciplinary efforts: the next frontier of photosynthesis research. *Frontiers in Plant Science*, **13**, 967203.

Author Query Form

Journal: TPJ

Article: 16098/2022

Dear Author,

During the copyediting of your manuscript the following queries arose.

Please refer to the query reference callout numbers in the page proofs and respond to each by marking the necessary comments using the PDF annotation tools.

Please remember illegible or unclear comments and corrections may delay publication.

Many thanks for your assistance.

AUTHOR: Please note that missing content in references have been updated where we have been able to match the missing elements without ambiguity against a standard citation database, to meet the reference style requirements of the journal. It is your responsibility to check and ensure that all listed references are complete and accurate.

Query reference	Query	Remarks